

PAPER • OPEN ACCESS

The Coupling of Grain Growth and Twinning in FCC Metals

To cite this article: Spencer L Thomas *et al* 2019 *IOP Conf. Ser.: Mater. Sci. Eng.* **580** 012026

View the [article online](#) for updates and enhancements.



ECS **240th ECS Meeting**
Digital Meeting, Oct 10-14, 2021
We are going fully digital!
Attendees register for free!
REGISTER NOW

The Coupling of Grain Growth and Twinning in FCC Metals

Spencer L Thomas¹, Jian Han^{2,4}, David J Srolovitz^{2,3,4*}

¹ Department of Materials Science and Engineering, North Carolina State University, Raleigh, NC 27695 USA

² Department of Materials Science and Engineering, University of Pennsylvania, Philadelphia PA 19104 USA

³ Department of Mechanical Engineering and Applied Mechanics, University of Pennsylvania, Philadelphia PA 19104 USA

⁴ Department of Materials Science and Engineering, City University of Hong Kong, Hong Kong SAR, China

* srol@seas.upenn.edu; srol@cityu.edu.hk

Abstract. Coherent twin boundaries (CTBs) routinely form during the annealing of polycrystalline metals, in the absence of an applied stress. Molecular dynamics (MD) simulations of normal grain growth in nanocrystalline metals show such annealing twins as well the formation of twin junctions. MD simulations and theoretical analyses demonstrate how these junctions form and that their formation necessarily retards grain boundary (GB) migration. Both CTB and GB migration occurs via disconnection motion. We identify the types of disconnections important for CTB migration and show the disconnection pile-ups at TJs during GB migration are responsible for CTB formation in the vicinity of TJs. Analysis further shows that at least two types twinning partials are to be expected during TJ migration and that these give rise to the multiple twinning near migrating TJs observed in the MD simulations.

1. Introduction

Twinning is common in a wide range of materials and especially in face centered cubic (FCC) metals. In FCC crystals, coherent twin boundaries (CTBs) are $\Sigma 3$ symmetric tilt grain boundaries (GBs) with a 60° rotation about a $\langle 110 \rangle$ axis and are typically associated with very low energy. If we describe the FCC crystal structure as a stacked sequence of $\{111\}$ planes, ...ABCABCABC..., a CTB may be described as a ...ABCAB**B**ACBA... (the CTB is at **B** here). CTBs commonly form during annealing or as a result of mechanical deformation and hence are often described as “annealing twins” or “deformation twins”: the two types of CTBs are structurally identical. Here, we examine how CTBs form, move, extend and, especially, are coupled to microstructure evolution (GB migration).

Grain boundaries migrate through the motion of line defects, that are constrained to move in the GB plane. These line defects, known as disconnections, have both dislocation (Burgers vector \mathbf{b}) and/or step (step height h) character. The set of possible disconnection modes $\{\mathbf{b}_m, h_m\}$ are fixed by bicrystallography; the important modes are determined by energetics and/or kinematics. Disconnection glide in the GB plane, translates the GB by a step height h and produces a shear displacement across the GB (i.e., displaces one crystal with respect to the other) by \mathbf{b} . Since CTBs are GBs, they too move by



disconnection motion. In most cases, the important disconnections for CTBs in FCC materials are $a/6 \langle 112 \rangle$ Shockley partial dislocations, where a is the cubic lattice parameter.

We report on a series of molecular dynamics simulations of grain growth in an FCC polycrystal, that show disconnection formation and extension in the absence of an applied stress. These simulations also demonstrate that formation of CTB penta-twin junctions (five twin GBs meeting along a common $\langle 110 \rangle$ axis) and other CTB junctions are a necessary result of GB migration in polycrystals. Most such junctions retard GB migration. Then, we examine the roles played by disconnections in CTB nucleation and CTB migration. The main conclusions of this report are (i) that CTB nucleation during annealing is a natural consequence of disconnection-mediated GB migration in polycrystals, (ii) that twin junction formation occurs naturally during grain growth, and (iii) that such junctions limit GB migration. This report is partially based on our previously published results [1-4].

2. CTB Formation and Extension during Grain Growth

We performed large-scale MD simulations of nanocrystalline nickel to study the atomistic features of grain growth using an EAM potential [5] and the LAMMPS MD simulation software [6]. The melting point for this potential, $T_m = 1590$ K, was determined using the phase coexistence method [7]. The simulations were performed under periodic boundary conditions in cubic simulation cells of edge length ≈ 40 nm and initial mean grain size ≈ 4.5 nm. The starting microstructures were generated using a continuum grain growth simulation method [8]; the widely applied Voronoi tessellation approach to generating grain growth microstructures yields (i) grain size distributions unrepresentative of normal grain growth [9], (ii) perfectly flat GBs, and (iii) unrealistic triple junction (TJ) angles. Each grain was populated with atoms arranged in a perfect face centered cubic (FCC) crystal of randomly-chosen orientation. Atoms significantly closer to one another than the equilibrium 0 K nearest neighbor distance were removed.

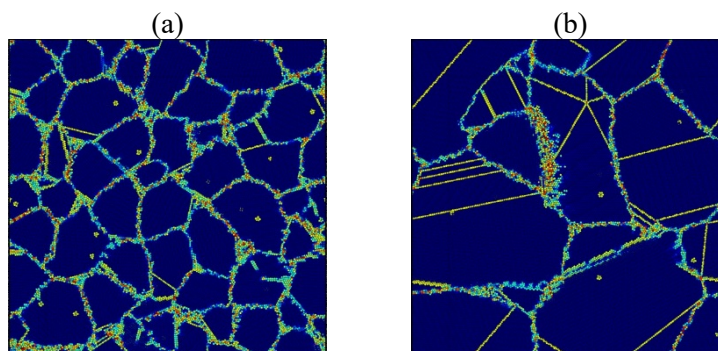


Figure 1. (a) Cross-section of the microstructure after initial relaxation and (b) after a 2.5 ns anneal. Atom colors are assigned based upon the centrosymmetry parameter. The thin, straight lines are CTB planes (with permission [1]).

Each initial atomic configuration was relaxed at 0 K using a conjugate gradient energy method and then MD annealed for 100 ps at 300 K to remove artifacts of the process that generated the initial configuration. A small number of twins were observed in the initial microstructure (see figure 1a). Annealing was performed in an NPT ensemble (Nosè-Hoover thermostat) for 2.5 ns with zero external stress at 1350 K ($\sim 0.85T_m$). The simulation time and temperature were chosen to be sufficiently for significant grain growth without grains spanning the simulation cell and without GB melting. Visualization was performed using the OVITO atomic visualization software [10].

Many coherent twin boundaries (CTBs) form during grain growth (see figure 1b). Nearly all CTBs form at migrating TJs, often in tightly-packed arrays (see figure 2) or in junctions between multiple twins and/or GBs (see figure 3). Preferential formation of CTBs at TJs mirrors experimental observations [11], but why twins form at migrating TJs remains an outstanding question.

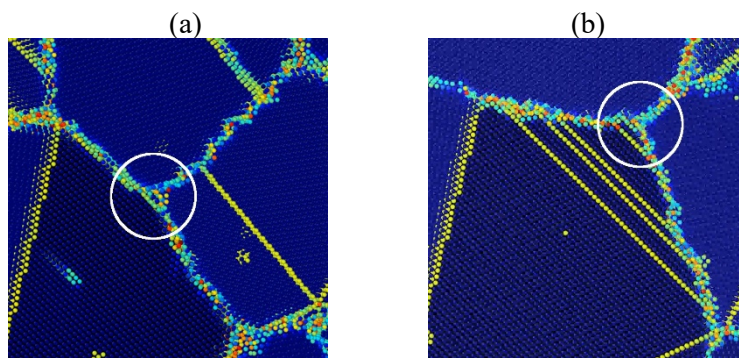


Figure 2. A series of twins emitted from a migrating TJ (circled in white).

Twin junctions have been observed to form in large networks during strain-engineered attention, with observations in nanowires [12,13], nanoparticles [14], and nanocrystalline (NC) metals (polycrystals with nanometer-scale grains) [15,16], but rarely in bulk coarse-grained materials [17]. The angle between CTB habit planes ($\{111\}$ in FCC) is $\theta_A = \arccos(1/3) \approx 70.53^\circ$, just short of the 72° required to restore a perfect, unstrained crystal. This closure failure implies that penta-twins have disclination character. As disclination stress fields grow linearly with distance from the disclination line, the elastic energy is too large to accommodate except in very small crystals and/or in nano-scale polycrystals.

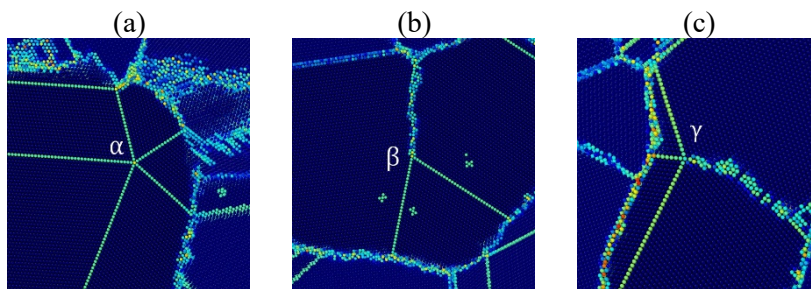


Figure 3. A penta-twin (α), a two CTB-GB junction (β) and three CTB-GB junction (γ) extracted from the nanocrystal grain growth simulation (with permission [1]).

CTB junctions arise naturally from GB migration in twinned grains. Consider a pair of twins on different planes intersecting a common GB. The CTBs extend as the GB migrates and eventually converge, leading to twin junction formation at the GB (see figure 4). As twins cannot terminate within a grain, the only possible CTB junctions consist of 5 twins (penta-twins) or two, three, or four CTBs and a GB; there are six distinct types of twin junctions - three are shown in figure 3 [1]. Twin junctions typically form along $\langle 110 \rangle$ axes in FCC metals.

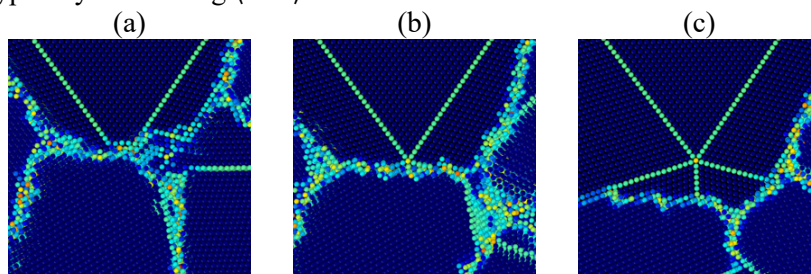


Figure 4. Penta-twin formed by collision of CTBs at a moving GB in a polycrystal (with permission [1]).

A migrating GB must form a twin junction to pull away from a 2-CTB collision (see Figs. 3 and 4). If the GB cannot form such a junction, it will be pinned, as in figure 5. Twin junction formation impedes GB migration as well, though this is less intuitive. Consider the formation of a new GB after a CTB collision (as in Figs. 3b and c). Further GB migration extends the new GB, increasing the energy of the system (proportional to the distance d from the junction to the original GB). As such, the junction

imposes a new driving force in opposition to GB migration, that is proportional to the new GB energy. The effect on grain growth can be understood in terms of the von Neumann-Mullins isotropic grain growth law [18,19], which states (in 2D) that the rate of grain area change is $\dot{A} = (M\gamma\pi/3)(n - 6)$, where M is the GB mobility, γ is the GB energy, and n is the number of GBs bounding the grain. For a shrinking grain, the effect of a (non-penta-) twin junction is to increase n by 1. This is significant; an initially 5-sided grain would cease shrinking entirely. Of course, this analysis of the effect on normal grain growth has been greatly simplified for clarity; including by the assumption of GB isotropy and the 2D nature of the analysis (this can be relaxed via the 3D extension of the von Neumann-Mullins expression [20]).

If a twin collision results in the formation of a penta-twin junction, the effect on the migration of the original GB is even more profound. This is because the penta-twin implies the existence of a disclination dipole (disclinations of strength $\omega = 2\pi - 5\arccos(1/3) \approx 7.356^\circ$ at the penta-twin core and the migrating GB). Further GB migration extends the dipole, resulting in a back force (per length parallel to the penta-twin) on the GB, $f(d) = -2K\omega^2d [1 + \ln(R/d)]$, where $K = \mu/4\pi(1 - \nu)$ (μ is shear modulus and ν is Poisson's ratio). If, however, the GB is perfectly slipping, the retarding force is $f(d) = -4\Lambda K\omega^2d [1]$ ($\Lambda = 0.593$ - numerical integration). In this case, the force retarding the motion of the original GB is proportional to the distance to the penta-twin; much like a spring, pulling the GB back to the penta-twin junction.

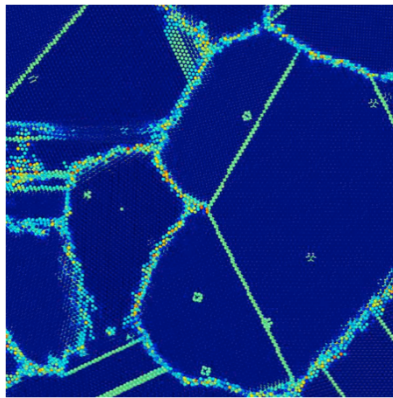


Figure 5. A GB pinned at a CTB collision point (center). The GB is severely distorted by the pinning junction (with permission [1]).

3. Disconnection description of CTB migration and CTB formation

Because CTBs are types of GBs, we can discuss GB and twin dynamics within the same mechanistic framework that is related to the crystal symmetry and the transformation that rotates one grain orientation into that of the grain across the GB. These symmetry considerations imply that there are line defects within the GB, known as disconnections [21,22,23], which have both dislocation and step character (i.e., a Burgers vector \mathbf{b} and step height h). When a disconnection glides along a flat GB, one grain translates with respect to the other (translation vector \mathbf{b}) and the GB migrates in the direction normal to the GB plane (by \mathbf{h}). This corresponds to coupled GB sliding and migration.

Analysis of the translational symmetry associated with the bicrystallography of a CTB reveals the character of CTB disconnections. Figure 6a shows a CTB, where the lattice points in the upper/lower grains are shaded black/white. To analyse the bicrystallography, we interpenetrate the two grains to form a dichromatic pattern (figure 6b). If we translate the black/white grains with respect to one another by the green vector \mathbf{b}_1 , the dichromatic pattern does not change, but the GB position shifts downwards by the blue vector \mathbf{h}_{10} (Figs. 6b and c). The green vector $\mathbf{b}_1 = [1\bar{1}2]a/6$ and blue vector $\mathbf{h}_{10} = -[\bar{1}11]a/3$ are the Burgers vector and step height associated with CTB disconnection 1. This type of CTB disconnection is also known as a twining partial [24].

We note that, by the same Burgers vector \mathbf{b}_1 (see Figs. 6b and c), the GB can also shift upwards by the step \mathbf{h}_{11} . This implies that the bicrystallography of a CTB allows multiple disconnection modes; they are characterized by \mathbf{b}_1 and $\mathbf{h}_{1j} = \mathbf{h}_{10} + j \Delta\mathbf{h}$, where $\Delta\mathbf{h} = [\bar{1}11]a$ and j is an integer. We can also choose

\mathbf{b}_2 (see figure 6b) as the Burgers vector of a disconnection, which has the same set of step heights as the disconnection with Burgers vector \mathbf{b}_1 . All possible CTB disconnection modes may be described as:

$$\mathbf{b}_1 = [1\bar{1}2]a/6, \mathbf{h}_{10} = -[\bar{1}11]a/3$$

$$\mathbf{b}_2 = -[211]a/6, \mathbf{h}_{20} = -[\bar{1}11]a/3,$$

where, in general, $\mathbf{b} = m\mathbf{b}_1 + n\mathbf{b}_2$, $\mathbf{h}_j = m\mathbf{h}_{10} + n\mathbf{h}_{20} + j\Delta\mathbf{h}$ and n, m and j are integers. The three twinning partials are $(\mathbf{b}_1, \mathbf{h}_{10})$, $(\mathbf{b}_2, \mathbf{h}_{20})$ and $(-\mathbf{b}_1 - \mathbf{b}_2, -\mathbf{h}_{10} - \mathbf{h}_{20} - \Delta\mathbf{h})$.

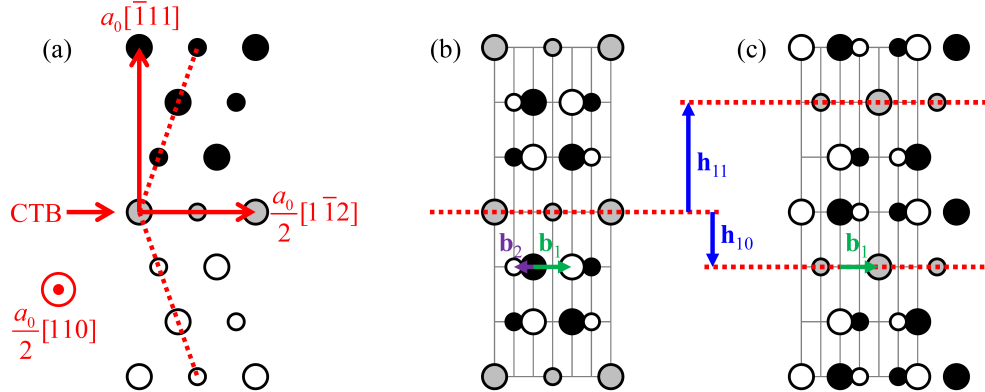


Figure 6. (a) CTB schematic. (b) Dichromatic pattern formed by interpenetration of upper (black) and lower (white) grains. Translation of the black with respect to the white grain by \mathbf{b}_1 produce pattern (c). The green vector denotes the Burgers vector of the CTB disconnection \mathbf{b}_1 and the purple vector denotes possible Burgers vector \mathbf{b}_2 . The blue vectors denote two possible step heights \mathbf{h}_{10} and \mathbf{h}_{11} associated with \mathbf{b}_1 .

Although many CTB disconnection modes are allowed by bicrystallography, they do not occur with equal probability. We expect that the most important are those associated with the lowest nucleation barriers. The nucleation barrier for disconnection mode (\mathbf{b}, \mathbf{h}) under shear stress (resolved to the CTB plane) τ and chemical potential jump ψ (across the CTB) driving forces may be estimated as [3]

$$E^* = 2\Gamma_s|h| + 2Kb^2 \ln\left(\frac{\delta^*}{ea}\right), \quad (1)$$

where Γ_s is the step energy and $\delta^* = 2Kb^2 / \tau \cdot \mathbf{b} + \psi h$ is the critical disconnection separation.

The nucleation barriers for a set of disconnections under a shear stress $\tau = 1$ MPa $\mathbf{b}_1/|\mathbf{b}_1|$ are shown in figure 7a, where we set $a = 3.615$ Å, $\Gamma_s = 0.59$ J/m² [25], $\mu = 28.05$ GPa, and $\nu = 0.35$ based on an EAM copper potential [26]. Since τ is parallel to \mathbf{b}_1 , $(\mathbf{b}_1, \mathbf{h}_{10})$ will be the most easily activated mode. The second lowest barrier modes correspond to the other two (energetically degenerate) twinning partials $(\mathbf{b}_2, \mathbf{h}_{20})$ and $(\mathbf{b}_3, \mathbf{h}_{30}) \equiv (\mathbf{b}_1 + \mathbf{b}_2, \mathbf{h}_{10} + \mathbf{h}_{20} + \Delta\mathbf{h})$. When a chemical potential jump $\psi = 1$ MPa is applied across the CTB, the most easily activated disconnection is a pure step. The modes with the second lowest barrier correspond to the three twinning partials. Operation of either the pure-step mode or the three twinning partial mode leads to CTB migration with no shear parallel to the CTB plane. These results show that CTB migration can be controlled by different disconnections depending on the nature of the driving force. Plastic deformation of the polycrystal can drive lattice dislocations into the CTB which may be viewed as heterogeneous sources for disconnection-mediated CTB migration.

As described above, the dynamics of both CTBs and more general GBs by the migration of disconnections. Disconnections modes for more general GBs are discussed in Ref. [3]. In polycrystalline material, GBs are not of infinite extent or extend across an entire sample but rather are terminated by triple junctions. The three GBs meeting at a TJ must migrate and/or slide cooperatively. Since the mechanism of GB migration/sliding is the motion of disconnections, the motion of the triple junction involve reactions between disconnections of the three GBs. Disconnection reactions during TJ motion has been observed in both experiments [27,28] and MD simulations [4].

If the disconnection reactions are such that there is a Burgers vector accumulation at the TJ, the associated stress field will repel additional disconnections from the TJ and migration must stop. The

condition that there is no net Burgers vector accumulation at the TJ can only be satisfied provided that the disconnection fluxes on the three GBs $J^{(i)}$ satisfy [3]

$$\begin{pmatrix} \mathbf{b}^{(1)} & \mathbf{b}^{(2)} & \mathbf{b}^{(3)} \\ h^{(1)}\sin\Theta^{(1)} & h^{(2)}\sin\Theta^{(2)} & h^{(2)}\sin\Theta^{(2)} \end{pmatrix} \begin{pmatrix} J^{(1)} \\ J^{(2)} \\ J^{(3)} \end{pmatrix} = 0, \quad (2)$$

where $\mathbf{b}^{(i)}$ and $h^{(i)}$ are the Burgers vector (column vector) and step height of disconnections on the i^{th} GB, and $\Theta^{(i)}$ is the dihedral angle opposite the i^{th} GB. The last row of this matrix corresponds to the condition that the three GBs meet at the TJ. Hence, effectively, we have 4 equations and 3 variables (the matrix is 4×3) and the only solution is that $J^{(i)} = 0$; i.e., there is no disconnection flux and no TJ migration. This implies that, in general, TJs cannot move and disconnections coming from the three GBs will accumulate/pile-up at the TJ and large TJ stresses will be generated at the TJ.

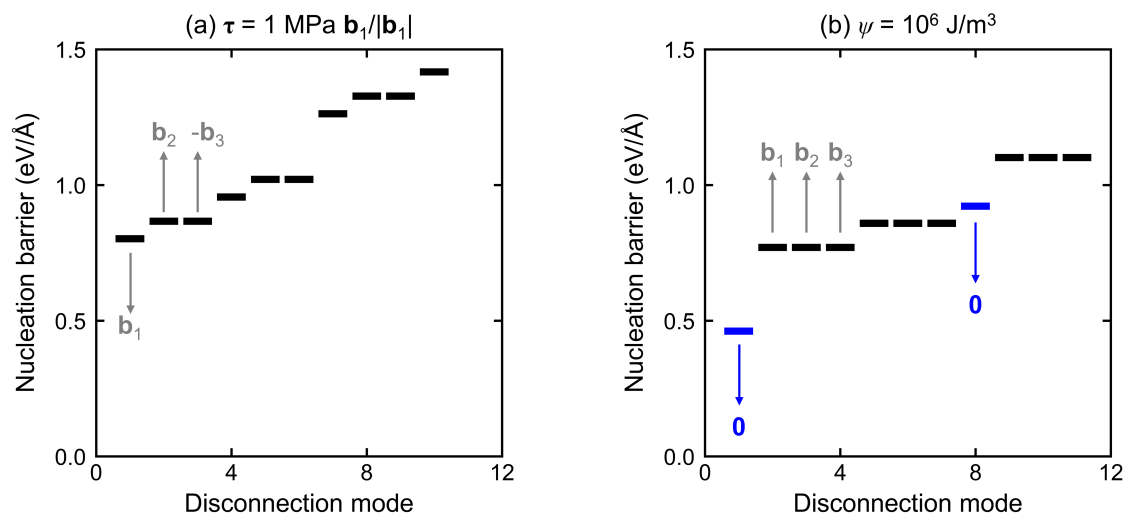


Figure 7. Nucleation barriers for a set of CTB disconnection modes: (a) CTB shear driven by a shear stress and (b) a CTB migration driven by a chemical potential jump.

Disconnection pile-ups at the TJs delimiting a GB may be described in the same manner as double-ended dislocation pile-ups. The stress-field at the end of such a pile-up at the TJ is proportional to the driving force for disconnection motion (if the GB were infinite) and the square root of the GB length (distance between TJs) L . If the driving force for disconnection migration is an applied stress τ then this gives the classical fracture mechanics result; i.e., the stress field at the TJ scales as $\sim \tau L^{1/2}$. If, on the other hand, the only driving force is capillarity (as in grain growth), then the stress field (associated with the disconnection pile-up) scales as $\sim \psi L^{1/2}$ (recall ψ is the jump in chemical potential across a GB). Since $\psi \sim \gamma \kappa$ (γ is the GB energy and κ is the mean GB curvature), $\kappa \sim 1/R$ (R is the grain size) and $L \sim R$, this implies that in grain growth there will be a stress generated at the TJ that $\sim \gamma/R^{1/2}$. In other words, grain growth generates large stresses at TJs and such stresses are larger in nanocrystalline materials than in large-grain polycrystals. Of course, nature abhors very large stresses, such those generated at the TJs in this manner. These stresses may be relaxed by formation of disconnections of other modes [3], dislocation plasticity within the grains or twinning (i.e., the formation of CTBs at the TJ).

We now consider twinning at the TJ as a means of relaxing the stress. Returning to the analysis of the TJ in terms of disconnections in Eq. (2), we now consider the possibility that the TJ may emit twinning partials dislocations. In particular, the fluxes of two twinning partials are associated with Burgers vectors \mathbf{b}^{T1} and \mathbf{b}^{T2} (i.e., J^{T1} and J^{T2}), such that

$$\left(\begin{array}{ccc|cc} \mathbf{b}^{(1)} & \mathbf{b}^{(2)} & \mathbf{b}^{(3)} & \mathbf{b}^{T1} & \mathbf{b}^{T2} \\ h^{(1)}\sin\theta^{(1)} & h^{(2)}\sin\theta^{(2)} & h^{(2)}\sin\theta^{(2)} & 0 & 0 \end{array} \right) \begin{pmatrix} J^{(1)} \\ J^{(2)} \\ J^{(3)} \\ J^{T1} \\ J^{T2} \end{pmatrix} = 0. \quad (3)$$

The matrix on the left is 4×5, corresponding to 4 equations and 5 variables (the 5 fluxes). Now, there is an infinite set of fluxes that can satisfy this equation (rather than no solutions other than $J^{(i)} = 0$ as before). Note, that if we only consider one type of twin, say T1, the matrix is 4×4 and the only solution would, again be all $J = 0$.

This result implies that if there is only one disconnection mode operating in each GB (typical for low temperature) and there is no dislocation plasticity within the grains, then (at least) two types of twins are required for general TJ (and, hence, GB) migration. This is consistent with the grain growth simulations shown in figure 1 where a series of twins were frequently observed near migrating TJs [1].

4. Conclusions

The formation of coherent twin boundaries (CTBs) during the annealing of face centered cubic metals (in the absence of an applied stress) is widely observed in experiments and atomistic simulations. The molecular dynamics simulations of normal grain growth presented here showed: (1) CTBs readily form during grain growth in the absence of an applied stress and span between grain boundaries, (2) CTBs on non-parallel $\{111\}$ that intersect a GB merge and form junctions as the GB migrates, (3) several types of junction form consisting of 2 or 3 CTBs and a GB or 5 CTBs in a penta-twin junction, and (4) sets of parallel CTBs often form at many migrating triple junctions (TJs). Theoretical analysis and MD simulations demonstrate that all CTB junctions retard (or stop) the migration of the GB from which the CTB junctions were formed and hence slow grain growth. Of the possible CTB junctions, penta-twin junctions are the most effective at retarding GB migration.

CTBs and more general GBs move via the migration of disconnections (line defects with both dislocation and step character) in their plane. The migration of CTBs can occur by disconnections motion that have twinning partial dislocation character or pure steps, depending on the nature of the driving force. The capillarity-driven migration of GBs during grain growth also occurs via the motion of disconnections. In a polycrystal, these disconnections pile-up at TJs creating large stresses in the vicinity of the TJs. Long-range TJ motion requires the relaxation of these stresses. This may occur via activation of higher energy disconnection modes, the emission/absorption of lattice dislocations, or twinning. In cases where the first two of these relaxation mechanisms do not operate (common in nanocrystalline metals), the large stresses associated with disconnection pile-ups lead to twinning at/near the migrating TJs. In cases where there is only one disconnection mode operating at the GBs meeting at the TJ, TJ migration requires at least two types of twinning modes (2 different twinning partials). This gives rise to the multiple twinning near migrating TJs observed in the MD simulations.

References

- [1] Thomas SL, King AH and Srolovitz DJ 2016 *Acta Mater.* **113** 301
- [2] Thomas SL, Chen K, Han J, Purohit PK and Srolovitz DJ 2017 *Nat. Comm.* **8** 1764
- [3] Han J, Thomas SL and Srolovitz DJ 2018 *Prog. Mater. Sci.* **98** 386
- [4] Thomas SL, Wei C, Han J, Xiang Y and Srolovitz DJ 2019 *Proc. Natl. Acad. Sci.* **116** 8756
- [5] Mishin Y, Farkas D, Mehl MJ and Papaconstantopoulos DA 1999 *Phys. Rev. B* **59** 3393
- [6] Plimpton S 1995 *J. Comp. Phys.* **117** 1
- [7] Puna GP and Mishin Y 2009 *Phil. Mag.* **89** 3245
- [8] Lazar EA, Mason JK, MacPherson RD and Srolovitz DJ 2011 *Acta Mater.* **59** 6837
- [9] Mason JK, Lazar EA, MacPherson RD and Srolovitz DJ 2015 *Phys. Rev. E* **92** 063308
- [10] Stukowski A 2010 *Model. Simul. Mater. Sci. Eng.* **18** 015012
- [11] Lin B, Jin Y, Hefferan C, Li S, Lind J, Suter R, Bernacki M, Bozzolo N, Rollett A and Rohrer R

2015 *Acta Mater.* **99** 63

- [12] Zhou GW, Zhang Z, Bai ZG, Feng SQ and Yu DP 1998 *Appl. Phys. Lett.* **73** 677
- [13] Wu B, Heidelberg A, Boland JJ, Sader JE, Sun X and Li Y 2006 *Nano Lett.* **6** 468
- [14] Hofmeister H 2004 *Fivefold twinned nanoparticles* in: *Encyclopedia of nanoscience and nanotechnology* (Stevenson Ranch: American Scientific Publishers) **3** 431
- [15] Wada T, Negami T and Nishitani M 1994 *Appl. Phys. Lett.* **64** 333
- [16] Narayan J, Srivatsa AR and Ravi KV 1989 *Appl. Phys. Lett.* **54** 1659
- [17] Wang W, Lartigue-Korinek S, Brisset F, Helbert AL, Bourgon J and Baudin T 2015 *J. Mater. Sci.* **50** 2167
- [18] von Neumann J 1952 *Metal interfaces*, ed C Herring (Cleveland: ASM) p 108
- [19] Mullins WW 1956 *J. Appl. Phys.* **27** 900
- [20] MacPherson RD and Srolovitz DJ 2007 *Nature* **446** 1053
- [21] Bollmann W 1970 *Crystal defects and crystalline interfaces* (Berlin: Springer)
- [22] Ashby MF 1972 *Surf. Sci.* **31** 498
- [23] Hirth JP and Balluffi RW 1973 *Acta Metall.* **21** 929
- [24] Anderson PM, Hirth JP and Lothe J 2017 *Theory of dislocations* (New York: Cambridge)
- [25] Bulatov VV, Reed BW and Kumar M 2014 *Acta Mater.* **65** 161
- [26] Mishin Y, Mehl MJ, Papaconstantopoulos DA, Voter AF and Kress JD 2001 *Phys. Rev. B* **63** 224106
- [27] Miura S, Hashimoto S and Fujii TK 1988 *Le J. Phys. Colloq.* **49** C5–599
- [28] Zhu Q, Cao G, Wang J, Deng C, Li J, Zhang Z and Mao SX 2019 *Nat. Comm.* **10** 156